https://doi.org/10.48047/AFJBS.6.Si3.2024.2001-2026

Swertiamarin and its analogues ameliorates diabetes-induced dyslipidemia by attenuating mitochondrial dysfunction through ACC-2 and CPT-1 signaling pathways

Shikha Goswami[1], Kalicharan Sharma[2], Ritu [1], Ramesh K Goyal[1]*[1] Department of Pharmacology, School of Pharmaceutical Sciences, DPSRU-110017[2] Department of Pharmaceutical Chemistry, School of Pharmaceutical Sciences, DPSRU-110017

Corresponding Author*:

Prof Ramesh K. Goyal

Department of Pharmacology, School of Pharmaceutical science, Delhi Pharmaceutical Science and Research University, New Delhi-110017
Email: goyalrk@gmail.com

Article Info

Volume 6, Issue Si3, 2024

Received: 19 April 2024

Accepted: 28 May 2024

doi: 10.48047/AFJBS.6.Si3.2024.

2001-2026

Abstract

The management of diabetes-induced dyslipidemia primarily focuses on ACC-2 and CPT-1 as key therapeutic targets. Dyslipidemia leads to impairment of mitochondrial function, which is intricately linked to the disruption of key enzymes ACC-2 and CPT-1, crucial in fatty acid synthesis and oxidation. Swertiamarin, which is an active constituent of *Enicostemma littorale* and has been reported to be effective in hyperglycemic condition. This prompted us to investigate the impact of Swertiamarin and its potent semi-synthetic derivatives in mitigating diabetes-induced dyslipidemia. Consequently, Swertiamarin analogues were designed and docked against the metabolic targets ACC-2 and CPT-1. To validate the docking results against the therapeutic targets, four compounds were selected for further synthesis and biological testing. Two compounds, SWL-2 and SWL-9 showed promising activity with IC_{50} values of 9.40 and 11.31 nM, respectively, against ACC-2 enzyme inhibition assay. In order to validate the potency and biological impacts of swertiamarin and its synthesized derivatives on the metabolic targets ACC-2 and CPT-1, a cell-based assay was performed using 3T3-L1 cells. Treatment with SWL-2 and SWL-9 (100ug/mL) showed better results compared to the standard (Metformin), as proven by a significant reduction in ACC-2 expression and an increase in CPT-1 concentrations. The findings of this study suggest that Swertiamarin and its derivatives have the potential to be used as lead compounds to manage dyslipidemia and other metabolic complications associated with diabetes.

Keywords:

Diabetes-induced dyslipidemia; Swertiamarin; Molecular docking; Semisynthetic analogues; Mitochondrial dysfunction, 3T3-L1 adipocytes

1. Introduction

Diabetes mellitus is a prevalent chronic metabolic disorder that has a substantial impact on a significant number of individuals globally. This condition gives rise to several complications that significantly affect the overall well-being of those affected. Among these complications, diabetes-induced dyslipidemia stands out as a major contributor to the increased cardiovascular risk observed in diabetes patients [1]. There is a complex relationship between diabetes and dyslipidemia that includes altered lipid synthesis and impaired lipid metabolism. However, the link between diabetes-associated dyslipidemia and its intricate relationship with mitochondrial function disruption and the imbalance of key enzymes, namely acetyl-CoA carboxylase-2 (ACC-2) and carnitine palmitoyltransferase-1 (CPT-1), remains a subject of ongoing investigation and scientific intrigue [2].

One of the key factors driving dyslipidemia in diabetes is increased hepatic lipid synthesis, specifically increased triglyceride and low-density lipoprotein cholesterol (LDL-C) levels. Insulin resistance, a hallmark of type 2 diabetes which encourages the activation of lipogenic pathways and increases the synthesis of fatty acids and triglycerides. Moreover, impaired lipid metabolism further exacerbates dyslipidemia in diabetes. Insulin resistance diminishes the activity of lipoprotein lipase, the enzyme responsible for the hydrolysis of triglycerides in circulating lipoproteins. It is debatable and unclear whether insulin resistance is caused by decreased or increased flow of long-chain fatty acids into the mitochondria [3]. Impaired mitochondrial uptake and oxidation of fatty acids are proposed as key factors leading to the development of insulin resistance, according to a prominent theory [4]. Carnitine palmitoyltransferase 1 (CPT-1) regulates mitochondrial beta oxidation and inhibited by malonyl-CoA, an acetyl-CoA carboxylase product (ACC). Data suggests that ACC-2, an isoform situated near CPT-1, is the primary regulator of CPT-1 activity. Hence, ACC-2 and CPT-1 are potential therapeutic targets for the treatment of metabolic syndrome [5]. In previous studies, it was found that long-chain acyl-CoAs (LC-CoAs) originating from lipids circulating in the body are directed away from carnitine palmitoyltransferase 1 (CPT-1). CPT-1 is a mitochondrial enzyme responsible for the initial and crucial step in the β-oxidation process of long-chain fatty acids. Instead, these LC-CoAs are preferentially utilized for the production of signaling molecules like diacylglycerol (DAG) and ceramide. Among the various fatty acid intermediates associated with the development of insulin resistance, long-chain acylcarnitines play a prominent role.

In general, higher concentrations of long-chain acylcarnitines have been considered an indication of incomplete mitochondrial processing of fatty acids, which triggers proinflammatory pathways associated with insulin resistance [6]. Over the past two decades, numerous comprehensive studies have yielded significant evidence that establishes a strong correlation between organ dysfunction and the abnormal accumulation of neutral lipids in diverse tissues, such as the heart, liver, pancreas, and skeletal muscle [7]. The controversy surrounding the role of fatty acid oxidation in regulating insulin sensitivity persists, and the underlying mechanisms remain unresolved. Carnitine palmitoyltransferase 1 (CPT-1), situated in the mitochondrial membrane, is

a vital enzyme in this process and is considered the limiting factor for the uptake of long-chain fatty acids into the mitochondria, where they undergo β-oxidation [8]. When animals are fed a high-fat diet, inhibiting CPT-1 with the compound etomoxir leads to increased lipid deposition and worsened insulin resistance [9]. Conversely, when CPT-1 is overexpressed, myotubes are protected against lipid-induced insulin resistance, suggesting that regulating the flux of fatty acids into the mitochondria is crucial in determining the effects of lipids on insulin sensitivity. The activity of CPT-1 in insulin-sensitive tissues is regulated by changes in the level of malonyl-CoA. Specifically, low levels of malonyl-CoA result in increased CPT-1 activity [10, 26]. The formation of malonyl-CoA occurs through the action of an enzyme called acetyl-CoA carboxylase (ACC), while the breakdown of malonyl-CoA is catalyzed by malonyl-CoA decarboxylase (MCD).

Understanding the complex mechanisms underlying diabetes-induced dyslipidemia is crucial for the development of effective therapeutic interventions aimed at ameliorating this major complication. Although there are multiple drug classes that provide supplementary and cumulative benefits in managing metabolic conditions such as Type 2 Diabetes Mellitus (T2DM) and insulin resistance [11], but a limited number of patients are able to achieve the recommended benefits for optimal insulin sensitivity. Additionally, it is uncommon for a normal physiological pattern of lipid oxidation to be restored. The urgent need for newer and more effective therapeutic approaches highlights the importance of addressing metabolic disturbances and their associated risks and complications. In several countries, herbal medicine has traditionally been used to manage metabolic disorders. Some Ayurvedic formulations containing *Enicostemma littorale* as an ingredient have demonstrated the ability to enhance insulin sensitivity in different models of insulin resistance [12] . *E. littorale* Blume, a smooth perennial herb from the Gentianaceae family, is commonly found throughout India, often in proximity to the sea. One of the primary compounds identified in *E. littorale* is swertiamarin, a secoiridoid glycoside. Previously, it has been reported that swertiamarin demonstrates noteworthy antihyperlipidaemic and hepatoprotective activity [13]. Consequently, our study aimed to further explore the impact of swertiamarin and its synthesized analogues on hyperlipidemia and insulin resistance, specifically targeting fatty acid metabolism in 3T3-L1 cells.

To address this hypothesis, we employed targeted metabolomics to evaluate the disruption of lipid-induced metabolic function in cell culture models [10]. Extensive research conducted supports the significant medicinal properties of swertiamarin, thus fulfilling the requirements of clinical networks in the development of new derivatives. Therefore, swertiamarin and its analogues show potential as viable drug options for managing dyslipidemia induced by diabetes. This aim of this study is to employ *in silico* and synthetic approaches to develop a novel molecule that selectively targets ACC-2 and CPT-1, with the goal of managing diabetes-induced dyslipidemia.

2. Experimental

2.1 *In silico* Work

It has been noted in previous studies that swertiamarin has a short plasma half-life [16]. To enhance the potency of swertiamarin, we designed and synthesized derivatives of swertiamarin to improve bioavailability and their anti-adipogenic properties. On the basis of Swertiamarin structure, we have designed 15 derivatives [**SI Figure 1**] of swertiamarin and docked against two targets ACC-2 (PDB ID: 3TDC) and CPT-1 (PDB ID: 1NM8) respectively for the identification of best fits. To enhance comprehension of the binding mode of Compounds (1-15) at the molecular level, we conducted molecular docking simulations of these compounds at the catalytic ligand binding sites of two receptors: Human Acetyl-CoA carboxylase 2 (ACC-2) (PDB ID: 3TDC) and Carnitine palmitoyltransferase 1 (CPT-1) (PDB ID: 1NM8). Docking simulations were performed using Maestro, version 9.6, which is a part of the Schrodinger software suite, for Compounds 1-15. The ligands were generated in a 3D format using the build panel and prepared for docking using the ligprep application [14]. The protein structure was obtained from the Protein Data Bank (PDB ID: 3TDC & 1NM8) for the docking study. The protein was prepared by eliminating solvent molecules, adding hydrogen atoms, and subjecting it to further minimization alongside a standard ligand using the protein preparation wizard. Molecular docking grids were generated based on the coordinates of the co-crystallized ligand. To validate the docking parameters, the co-crystallized ligand was docked again into the protein's catalytic site. The root-mean-square deviation (RMSD) between the standard and re-docked poses was calculated and found to be 0.765 Å for ACC-2 and 0.865 Å for CPT-1. Compound (1-15) was docked using the Glide extra-precision (XP) mode, which saves up to three poses per molecule.

Based on molecular docking results, analogues SWL-1, SWL-2, SWL-9 and SWL-15 selected for further synthesis. Out of the best-chosen compounds, SWL-1 is Swertiamarin itself. Substitutions in swertiamarin (SWL-1) had higher hydrophobic interactions with the receptor sites and this may also have been attributed to the increase in activity.

2.2 Chemistry

Whole plant material of *Enicostemma littorale* was collected from Tamilnadu (India). The identification of the plant was based on its morphological and microscopical characteristics, as described in various authoritative texts and floras by the NISCAIR department in New Delhi, India. The chemicals utilized for synthesis, including 9-Borabicyclo 3.3.1 nonane 0.5M tetrahydrofuran (9-BBN), Hydrogen Peroxide, Standard swertiamarin, and Dry dimethylformamide (DMF), were procured from Sigma-Aldrich. Melting points were determined using a digital melting point apparatus called 'VEEGO' through the open capillary method. 1H NMR spectra were recorded on a Bruker avance neo 500 MHz NMR spectrometer at SAIF, P.U. Chandigarh, employing DMSO as the solvent and TMS as an internal standard. Mass spectral analysis was conducted using the Waters Q-TOF micromass (ESI-MS) instrument at SAIF/CIL, P.U. Chandigarh. The progress of reactions was monitored via TLC using pre-coated silica gel aluminum plates (Kiesel gel 60, 254, E. Merck, Germany), and the zones were observed visually

under ultraviolet irradiation. The purity of the final compounds was assessed using chromatographic systems.

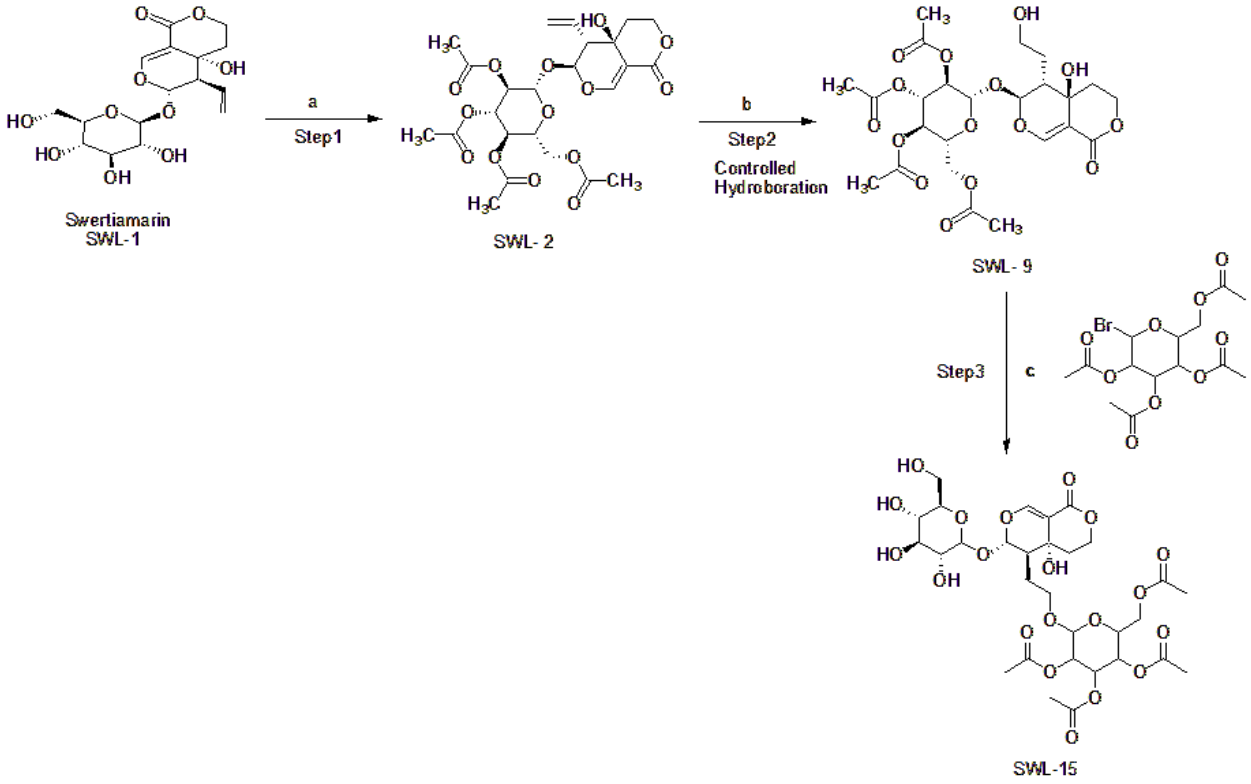

Figure 1: Synthetic scheme for SWL-1, SWL-2, SWL-9 and SWL-15, **a)** Ac_2O, Pyridine at 0-8℃ and the temperature to be raised up to 37℃ for 24 h, b) 0.5 M solution of 9- BBN, dry THF, 3 N NaOH , H_2O_2 (30% aq.) and maintained at 37℃ for 6 h, c) 2,3,4,6- tetra-O-acetyl alpha-D-glucopyranosyl bromide, dry DMF; Cs_2CO_3 in presence of Pd_2db_3 catalyst and maintained the reaction at 37℃ for 16 h.

2.2.1 Isolation of Swertiamarin (SWL-1)

The extraction and characterization of swertiamarin (SWL-1) were performed following a previously published method [15]. The isolation process was conducted in accordance with the mentioned procedure. Following isolation, the resulting precipitate was filtered and subsequently rinsed using ethyl acetate.

Pale yellow, yield = 6.5%, Melting point =112- 114°C; ^{1}H NMR (500 MHz, DMSO) chemical shift values (δ): 1.73 (2H, m, CH_2); 2.83 (1H, m, CH); 3.81 (1H, m, CH); 4.28 (1H, m, CH); 5.25 (1H, m, CH); 5.35 (2H, d, CH_2); 5.63 (1H, s, CH); 7.54 (1H, s, CH); and glycan hydroxyl groups: 2.82 (1H, t, CH); 3.03 (1H, m, CH), 3.15 (2H, m, CH_2), 3.43 (1H, m, CH); 3.67 (1H, m, CH); 4.45 (1H, d, CH); ESI- MS m/z found 374.1761, Calcd 374.34.

2.2.2 (2R,3R,4S,5R,6S)-2-(acetoxymethyl)-6-(((3S,4R,4aR)-4a-hydroxy-8-oxo-4-vinyl 3,4,4a, 5,6,8-hexahydropyrano[3,4-c] pyran-3-yl) oxy) tetrahydro-2H-pyran-3,4,5-triyl triacetate (SWL-2)

The synthesis of SWL-2 was carried out through **scheme 1**. Swertiamarin (0.53 mM) was dissolved in 5ml of dry dimethylformamide (DMF) and stirred for 5 minutes at 0-8℃. Pyridine (2.1 mM) was added as a base during the stirring process, followed by the gradual dropwise addition of acetic anhydride (2.1 mM) [16]. The progress of the reaction was verified using thin-layer chromatography (TLC). After the reaction finished, the mixture obtained was carefully transferred into crushed ice and subjected to two extractions using 6 ml of diethyl ether each time. The diethyl ether was subsequently removed by evaporation under reduced pressure, and the residue was rinsed with hot water. The purification of compound was done by using flash chromatography with mobile phase DCM: MeOH (9:1) and silica gel G was used for reusable column.

White compound, yield = 84%, Melting point =188-190°C; ^{1}H NMR (500 MHz, DMSO) chemical shift values (δ): 1.76 (2H, m, CH_2);1.82(2H, d, CH_2); 2.02-2.14 (12H, d Ac*4); 2.83 (1H, d, CH); 3.81 (2H, d, CH_2); 4.12 (1H, m, OH); 4.28 (2H, m, CH_2); 4.89 (1H, d, CH); 5.1 (1H, d, CH); 5.23 (1H, m, CH); 5.35 (3H, m, CH_3); 5.63 (1H, s, CH); 7.54 (1H, s, CH); ESI- MS m/z $[M+H]^+$ found 543.1372, Calcd 542.48.

2.2.3 (2R,3R,4S,5R,6S)-2-(acetoxymethyl)-6-(((3S,4R,4aR)-4a-hydroxy-4-(2-hydroxyethyl)-8-oxo-3,4,4a,5,6,8-hexahydropyrano[3,4-c]pyran-3-yl)oxy)tetrahydro-2H-pyran-3,4,5-triyl triacetate (SWL-9)

The hydroboration reaction was carried out with SWL-2 for the synthesis of SWL-9. In RBF 9-Borabicyclo 3.3.1 nonane 0.5M tetrahydrofuran (9BBN, 14.5 mM, 1 equiv.) was taken in dry THF followed by addition of H_2O_2 (30% aqueous, 0.3 mL) and 3M NaOH (to maintain pH 8) subsequently. The reaction was initiated with a N_2 blanket, and subsequently, the temperature was gradually increased from 0–8℃ until it reached 37℃ over a period of 6 hours **(scheme 1)**. The progress of the reaction was observed using thin-layer chromatography (TLC). Once the reaction was finished, it was cooled down by adding ice and then neutralized with dilute hydrochloric acid (HCl). The resulting mixture was extracted using ethyl acetate to obtain the crude compound. Compound was purified by flash chromatography by taking 100-200 silica and DCM-MeOH mobile phase [17].

White Yellow, yield =51%, Melting point =109-111°C; ^{1}H NMR (500 MHz, DMSO) chemical shift values (δ): 1.64 (2H, d, CH_2); 1.83 (4H, m, $2CH_2$); 2.02-2.14 (12H, d, Ac*4); 2.83 (1H, d, CH); 3.81 (2H, d, CH_2); 4.12 (2H, d, 2OH); 4.28 (2H, m, CH_2); 4.89 (1H, m, CH); 5.1 (1H, d, CH); 5.23 (1H, m, CH); 5.35 (3H, m, CH_3); 5.63 (1H, s, CH); 7.54 (1H, s, CH); ESI- MS m/z $[M+H]^+$ found 562.6315, Calcd 560.5.

2.2.4 (4aR,5R,6S)-4a-hydroxy-5-(((3R,4R,5S,6R)-3,4,5-trihydroxy-6-(hydroxymethyl)tetrahydro-2H-pyran-2-yl)methyl)-6-((3R,4S,5S,6R)-3,4,5-trihydroxy-6-(hydroxymethyl) tetrahydro-2H-pyran-2-yloxy)-4,4a,5,6-tetrahydropyrano[3,4-c]pyran-1(3H)-one (SWL-15)

Compound SWL-9 were dissolved in RBF containing 2,3,4,6- tetra-O-acetyl alpha-D-glucopyranosyl bromide and 5mL of dry dimethylformamide (DMF) followed by Cs_2CO_3 (3 equiv.), pd_2dba_3 (0.1 equiv.) and continue the reaction with a blanket of N_2 at 0°C - 8°C for 1h **(scheme 1)**. Subsequently, the temperature gradually raised to 37°C over 16 hours. After the reaction was completed, the reaction mixture was acidified using HCl and then subjected to extraction with ethyl acetate. The organic layer was subsequently dried using sodium sulfate.

The synthesis of SWL-15 was unsuccessful due to synthetic challenges, as evidenced by the Mass and NMR data. We have tried so many trial with different routes and reaction conditions but unable to get the desired product.

2.3 Biological evaluation

2.3.1 Reagents

Swertiamarin was previously isolated and stored from the whole dried plant of *Enicostemma littorale*. Metformin was a gift sample from Zydus Cadila (Ahmadabad, India). Insulin, Oleic acid, Dimethylsulphoxide (DMSO), Dulbecco's Modified Eagle's Medium (DMEM) and Dexamethasone (DEX) were purchased from Sigma Aldrich, USA. Foetal Bovine Serum (FBS), amphotericin-B, trypsin, penicillin-streptomycin, and calf serum were obtained from Gibco (USA). Other reagents were: Triglycerides, ACC-2 and CPT-1 ELISA assay kit purchased from (ELK Bitechnology Cat: ELK7024 and Cat: ELK9786).

2.3.2 ACC inhibition assay

The ACC-2 inhibitory activity of synthesized analogues was estimated using the The ADP-Glo™ kinase assay. Briefly, a working solution having recombinant ACC-2 (BPS Biosciences, 50201) and a diluted compound solution were mixed in a 96-well Optiplate (Perkin Elmer, 6007290, USA) and left to incubate at room temperature for 15 minutes. Subsequently, a substrate mixture was added to initiate the reaction, and the plate was incubated for 60 minutes at room temperature. After that, ADP-Glo reagents were added and the plate was incubated for an additional 40 minutes to deplete the remaining ATP. Lastly, kinase detection reagents were introduced and incubated for 40 minutes to convert ADP to ATP. The luminescent signal of ATP was measured using an Envision multifunction reader (BioTek Synergy LX Multi-Mode Microplate Reader, USA) [18]. The IC_{50} values were calculated based on the obtained data.

2.3.3 Cell Culture and adipocytes differentiation

3T3-L1 cell line used for *in vitro* study was procured from the National Centre for Cell Science (NCCS), Pune, India. The 3T3-L1 preadipocytes were incubated at 37°C with 5% CO_2 in DMEM medium containing 10% fetal bovine serum (FBS), 100 U/ml penicillin, and 100 µg/ml streptomycin until they reached confluence. Two days after reaching confluence, the cells were differentiated using the following substances: Oleic acid (0.5 mM), Insulin (10 µg/ml) and Dexamethasone (390 ng/ml). This differentiation process was performed in DMEM containing 10% FBS, as described in previous studies [19]. The concentrations of Oleic acid, Dexamethasone, and insulin were determined by referring to a dose-response curve that had been established through preliminary experiments. Furthermore, the cells were treated with SWL-1, SWL-2 and SWL-9 at a concentration of 100 µg/ml, either in the presence or absence of the differentiation substances. These compounds were dissolved in DMSO for treatment purposes. Control cells were treated with a vehicle solution consisting of DMSO at a concentration of 0.05%, while untreated cells received only the media without any additional treatment (referred to as NC). After 48 hours of treatment, the medium was changed to DMEM containing 10 µg/ml insulin, 10% FBS and the respective treatments were continued. The medium was replaced every 48 hours until day 10. On the 10th day, the fully differentiated adipocytes were subjected to Oil Red O staining to assess lipid accumulation within the cells. Intracellular triglyceride levels were also measured, and protein analysis was conducted as part of the study.

2.3.4 Cell viability/ Cytotoxicity assay

Cell viability was assessed using an MTT assay with minor modifications [20]. 3T3-L1 preadipocytes were cultivated in 96-well microtiter plates at a density of 10,000 cells per well and incubated for 24 hours. Subsequently, they were treated with various concentrations of SWL-1, SWL-2, and SWL-9 (10, 50, 100, 250, and 500 µg/ml) or left untreated. After 24 hours, the media was discarded and 20 µl of MTT solution (5 mg/ml) was added to each well. The cells were then incubated at 37°C for 2 hours. After the incubation period, the MTT solution was eliminated, and the formazan crystals were dissolved in 100 µl of DMSO. The resultant solution with color was measured at 570 nm to determine the cell viability, expressed as a percentage compared to the control group [21].

2.3.5 Oil Red O staining and triglycerides assay

The quantification of lipid accumulation in adipocytes involved two methods: the triglyceride assay and the Oil Red O staining method [20]. The cells were washed thrice with 1X phosphate-buffered saline (PBS) after removing the culture medium. Oil Red O dye was then applied and incubated for 15 minutes at room temperature. After rinsing the adipocytes, we captured an image. To examine the accumulation of triglycerides within adipose cells, we conducted lipid extraction from differentiated adipocytes. In brief, the cells were rinsed with 1X PBS, scraped using PBS, and then centrifuged at 1500 rpm for 5 minutes. The resulting cell pellet was resuspended in 1 ml of 1X PBS, and the lipids were subsequently extracted. These extracted

lipids were dissolved in isopropyl alcohol to measure triglyceride levels, and the obtained data were presented as Mmol of triglycerides.

2.3.6 Extraction of cell lysates from differentiated 3T3-L1 cells

Protein extraction was performed from differentiated 3T3-L1 cells to investigate the impact of swertiamarin and its synthesized analogues on ACC-2 and CPT-1. Carefully remove the culture medium from the differentiated 3T3-L1 cells by decanting it. Ensure the cells are thoroughly washed twice with cold PBS, followed by gentle detachment using trypsin, and collected through centrifugation at 1000× g for 5 minutes. Perform three additional cold PBS washes on the cells. Afterward, resuspend the cells in a fresh lysis buffer with a concentration of 10^7 cells/ml. If required, ultrasonication can be applied until the solution is clarified. Centrifuge the mixture at 1500 × g for 10 minutes at 2-8℃ to eliminate cellular debris. Transfer the resulting supernatant to a new tube for further analysis [22].

2.4 ELISA based assay estimation for ACC-2 and CPT-1

The measurement of ACC-2 and CPT-1 assays was carried out on cell lysates extracted from differentiated 3T3-L1 cells for swertiamarin and its synthesized analogues for the evaluation of anti-diabetic potential. Estimation was done by particular ELISA kits (Purchased from ELK Biotechnology) by using multi-mode reader as per the manufacturer method. The test in this kit follows the sandwich enzyme immunoassay principle. The microtiter plate is included, already coated with antibodies specific to ACC-2 and CPT-1. Following that, Avidin conjugated to HRP is introduced to each well and incubated. When the TMB substrate solution is applied, only those wells containing ACC-2 and CPT-1, along with biotin-conjugated antibody and enzyme-conjugated Avidin, will display a color change. The enzyme substrate reaction concludes with the addition of a sulphuric acid solution, and the resulting color change is measured spectrophotometrically at a wavelength of 450 ± 10nm. To ascertain the concentration of ACC-2 and CPT-1 in the samples, their OD is compared to the standard curve, allowing for accurate quantification.

2.5 ADMET and MM/GBSA Study

The synthesized compounds underwent ADMET analysis using QikProp (Version 3.5). QikProp offers a comparison of a specific molecule's properties with those of 95% of established drugs [14]. The calculated properties of the compounds included various descriptors such as the partition coefficient, CNS activity, human oral absorption and gut-blood barrier permeability. In order to evaluate the binding affinity of the synthesized compounds with 3TDC and 1NM8, we employed MM/GBSA energy calculations using the Prime module of the Schrödinger molecular modeling package.

2.6 Statistical analysis

The data was subjected to analysis using one-way and/or multifactor one-way analysis of variance (ANOVA) to ascertain its level of significance. The results are presented as Mean ± SEM. Statistical significance was denoted by * for $P < 0.05$, ** for $P < 0.01$, and *** for $P < 0.001$.

3. Results

3.1 Molecular docking

The docking studies reveal a common binding orientation of Compounds (1-15) within the catalytic binding pocket of the Human Acetyl-CoA carboxylase 2 receptor (PDB ID: 3TDC) and Carnitine palmitoyltransferase 1 (PDB ID: 1NM8). Herein, we report the binding pose of highest scoring compounds and compare them with the standard co-crystallized ligand which was docked against ACC-2 and CPT-1 protein **(Table-2)**. All Compounds (1-15) binds in catalytic domain of Human Acetyl-CoA carboxylase 2 and Carnitine palmitoyltransferase 1 receptor. Highest scoring compounds SWL-2, SWL-9 and SWL-15 binding interaction (Hydrogen Bonding) with backbone of ACC-2 and CPT-1 receptor listed in **Table 1 (Figure 2&3)**. Highest docking scoring compound (SWL-15) superimposition with standard ligand (Metformin) and showed same interaction was found in catalytic domain of Human ACC-2 and CPT-1. Docking score of Compounds (1-15) were also similar with Standard ligand.

Table 1: Binding interactions of highest scoring compounds with catalytic domain of ACC-2 and CPT-1

S.N.	Compound Code	Interactions against ACC-2	Interactions against CPT-1
1.	SWL-2	H-bonds-Gly1986	H-bonds- Thr446
2.	SWL-9	H-bonds-Gly1986, Leu1984, Ile1860,Ile1963	H-bonds-Thr444 and Thr446
3.	SWL-15	H-bonds-Thr1985, Leu1984 and Ala1858	H-bonds-Ser531, Ser533, Met526, Glu326 and Gly327
4.	Metformin	H-bonds-Thr1985, Ala1989	H-bonds-Gly327 and Glu326

A1	**A2**
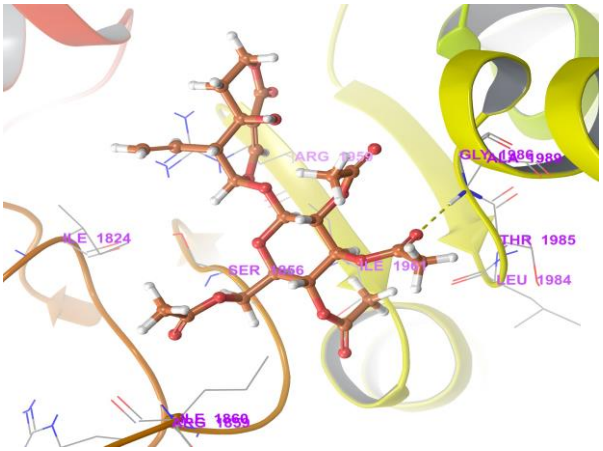	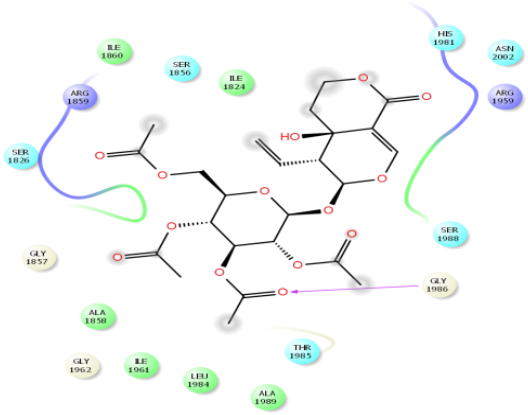
A3	**A4**
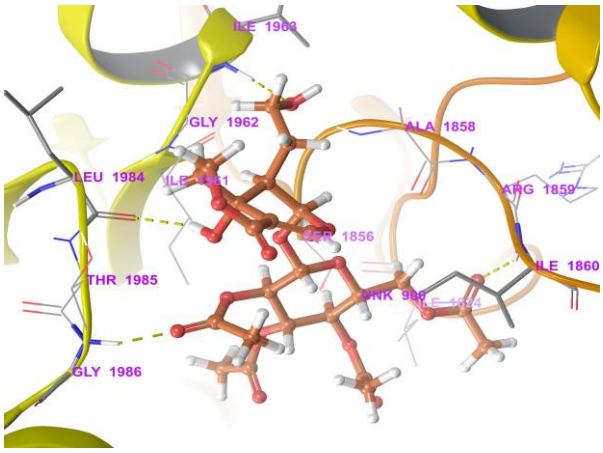	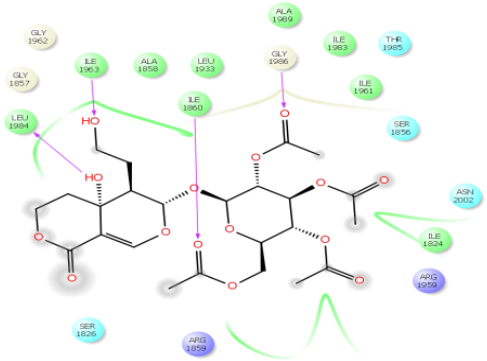
A5	**A6**
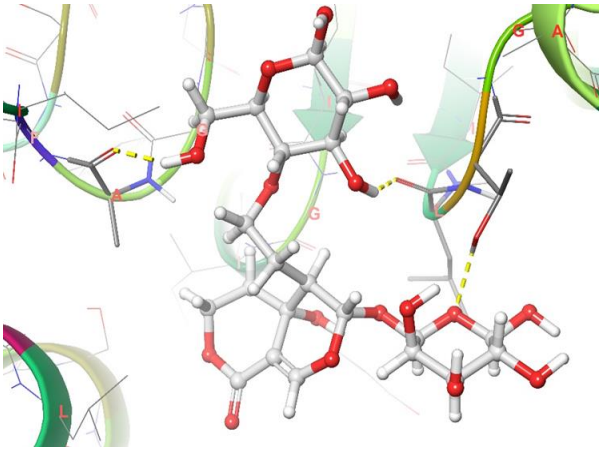	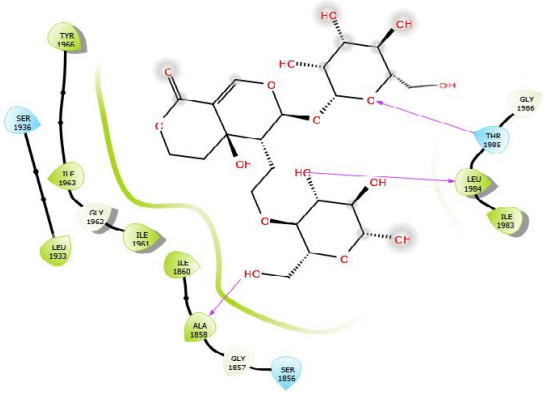
A7	**A8**

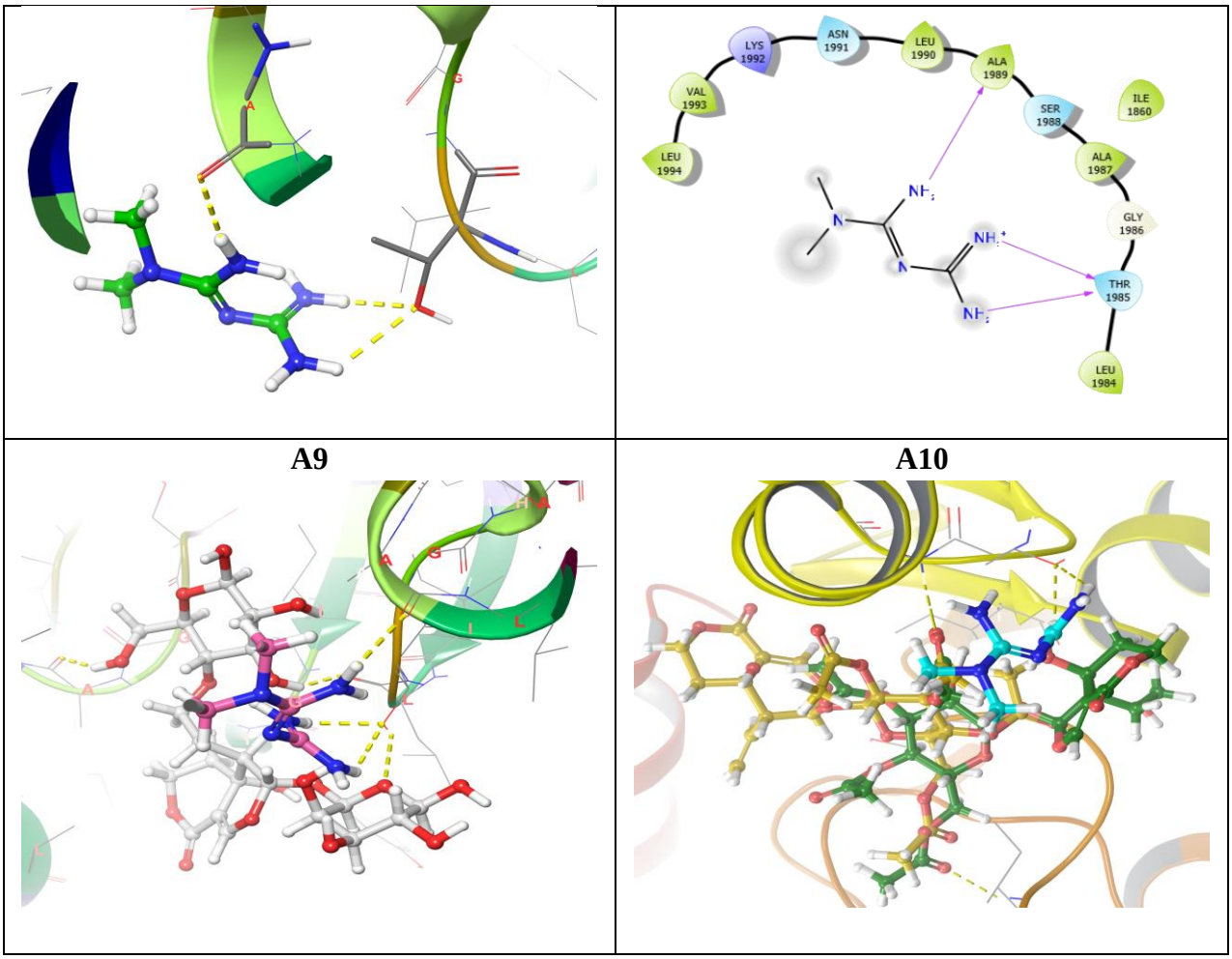

Figure 2: A1, A3, A5 docking pose of highest scoring compounds SWL-2, SWL-9 and SWL-15 in human ACC-2 receptor active site, **A2, A4, A6** ligplot of highest scoring compound SWL-2, SWL-9 and SWL-15 against human ACC-2 active site, **A7** & **A8** docking pose and ligplot of standard ligand Metformin against human ACC-2 active site, **A9** superimposition of highest scoring compound SWL-15 at catalytic domain of human ACC-2 with standard ligand **& A10** superimposition of highest Scoring compounds SWL-2 and SWL-9 at catalytic domain of human ACC-2 with standard ligand.

B1	**B2**
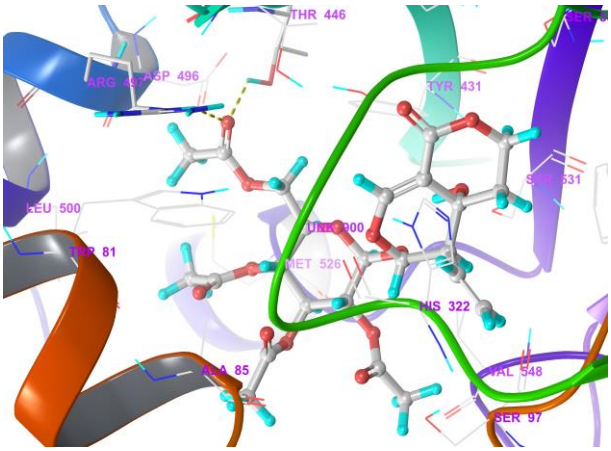	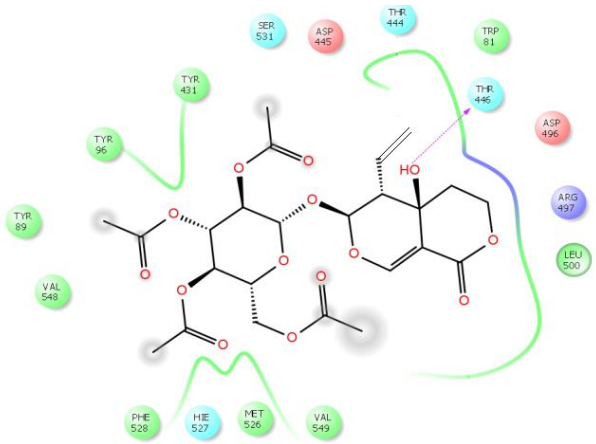
B3	**B4**
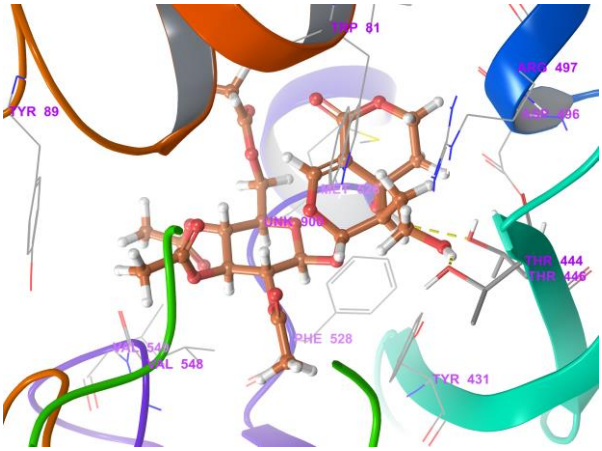	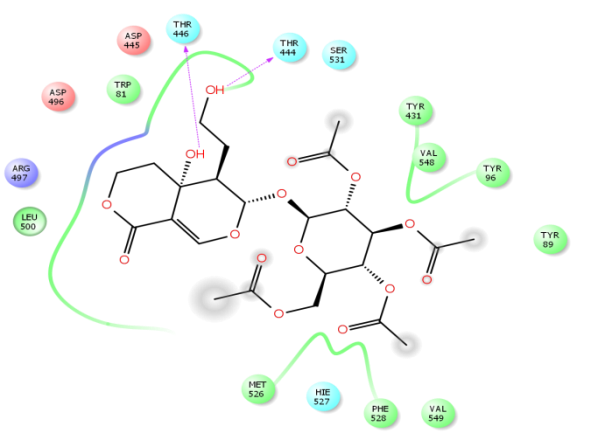
B5	**B6**
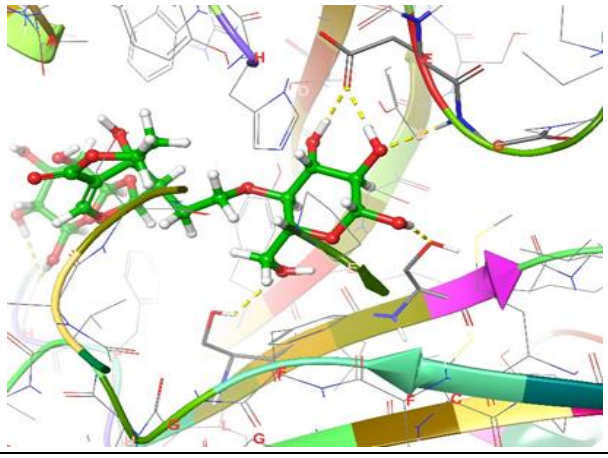	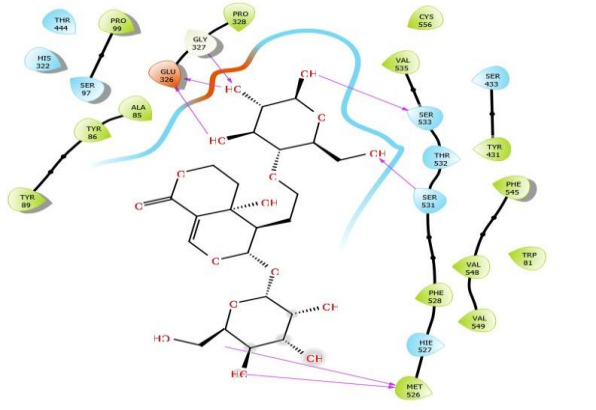
B7	**B8**

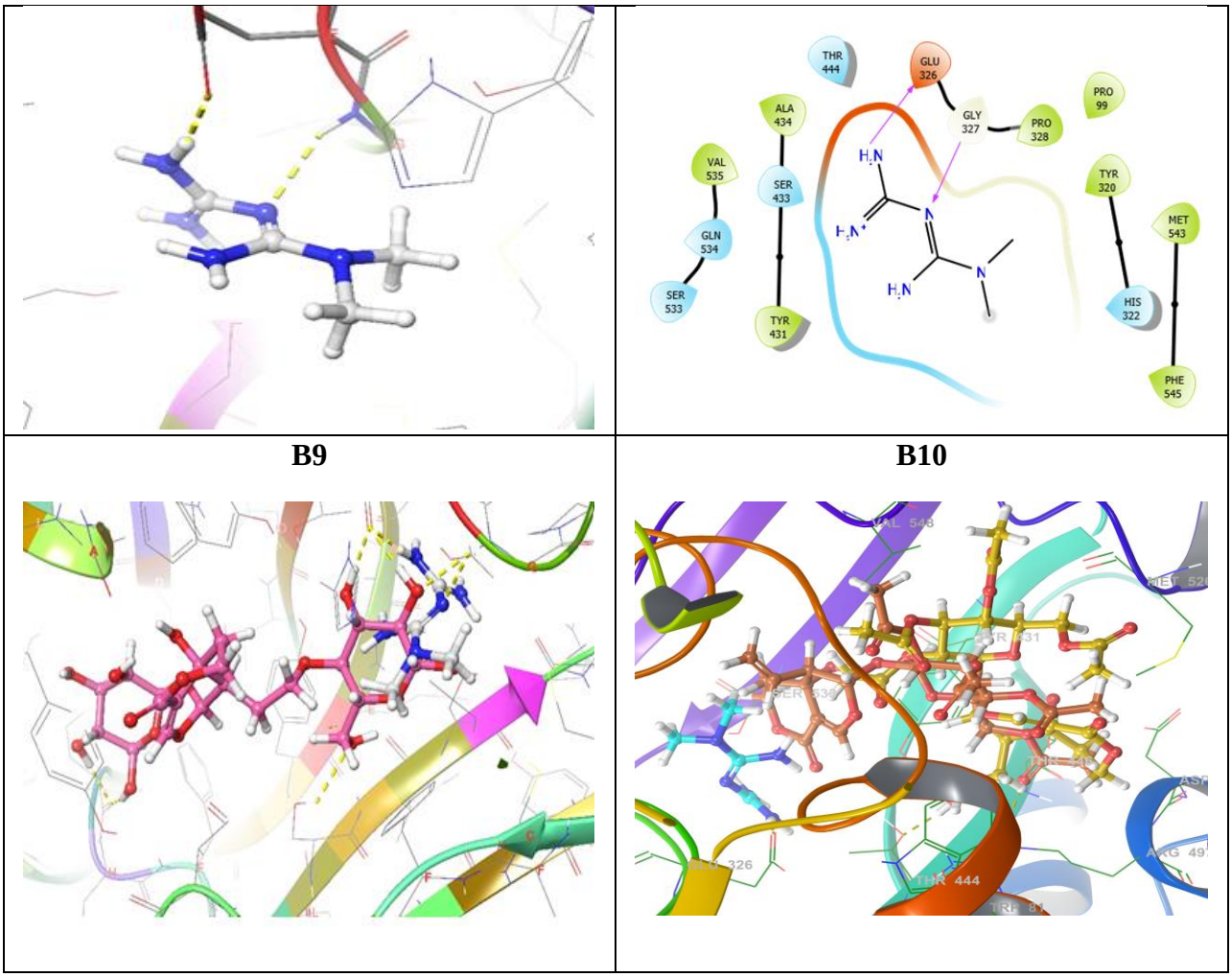

Figure 3: B1, B3, B5 docking pose of highest scoring compounds SWL-2, SWL-9 and SWL-15 in human CPT-1 active site, **B2, B4, B6** ligplot of highest scoring compounds SWL-2, SWL-9 and SWL-15 against human CPT-1 active site, **B7 & B8** docking pose and ligplot of standard ligand Metformin against human CPT-1 active site, **B9** superimposition of highest scoring compound SWL-15 at catalytic domain of human CPT-1 with standard ligand **& B10** superimposition of highest scoring compounds SWL-2 and SWL-9 at catalytic domain of human CPT-1 with standard ligand.

Table 2: Binding score of Swertiamarin analogues in reference to standard

S.N.	Receptor Used	PDB-ID	Control Used	Control Binding Score	Swertiamarin and analogues binding score			
					SWL-01	SWL-02	SWL-09	SWL-15

1.	ACC-2 – Acetyl-CoA carboxylase (CT) domain	3TDC	(CP-640186) & Metformin	-1.044 & -0.412	-6.067	-7.15	-6.162	-7.255
2.	CPT-1 Carnitine Palmitoyl transferase I	1NM8	L-Carnitine & Metformin	-4.12 & -1.629	-9.442	-9.374	-9.381	-11.469

Four of the best-fitting compounds out of 15 designed and docked analogues were ultimately selected for further synthesis. Out of the four analogues, SWL-1 was swertiamarin by itself. Out of the remaining molecules, successful synthesis was achieved for SWL-2 and SWL-9. The synthesized molecules were subjected to further analysis for confirmation and purity using NMR and mass spectrometry techniques.

3.2 Characterization of isolated swertiamarin and its synthesized analogues

Swertiamarin (SWL-1) was isolated from *Enicostemma littorale* plant as per the reported method. Subsequently, SWL-1, SWL-2, and SWL-9 were subjected to characterization through the application of Mass and NMR spectroscopic techniques. The yield for SWL-1, SWL-2 and SWL-9 after derivatization of swertiamarin was found to be 6.5, 84 and 51%, respectively. The melting points of SWL-1, SWL-2 and SWL-9 were found to be 112-114°C, 188-190°C and 109-111°C, respectively. The synthesized derivatives of swertiamarin were confirmed to have molecular weights through the observation of a molecular ion peak (m + 1) at 543.13 for SWL-2 and 562.63 for SWL-9 in the mass spectra. Additionally, the proton NMR spectra of all compounds indicated a downfield shift of tertiary and secondary alcohol protons, providing confirmation that esterification of sugar alcoholic protons was effectively executed [**Refer to SI; Figure 2-4**].

3.3 *In vitro* results

3.3.1. *In vitro* ACC inhibitory activity

In vitro enzymatic inhibitory effects of Swertiamarin and synthesized analogues were evaluated. The preliminary screening was carried out at two concentrations (10 and 50 µM), where CP-640186 and Metformin were selected as the positive control. As shown in Table 5, Swertiamarin (SWL-1) exhibited weaker hACC-2 inhibitory activity than SWL-2 and SWL-9. Among all the analogues, compound SWL-2 appeared to be the most potential ACC-2 inhibitor at 50 µM.

Acetylation of SWL-1(Swertiamarin) to synthesize SWL-2 shows better enzymatic activity, wherein compound SWL-2 exhibited the most potent ACC inhibitory effect, which can be partly

attributed to the presence of its bulky Acetyl group. Additionally, the inhibition ratio (IR) values of SWL-9 was slightly lower than of SWL-2. These findings suggest that introducing Acetyl groups or incorporating bulky functional groups at the right-hand polar end of the molecule promotes ACC inhibition.

Based on the above results, the IC_{50} values of the synthesized compounds were calculated and summarised in **Table 3**. The IC_{50} value of SWL-2 on the hACC-2 enzyme was 9.40 nM, which was comparable to positive standards CP-640186 and Metformin (IC_{50} 5.67 and 6.09 nM respectively).

Table 3: The ACC-2 inhibitory activity of Swertiamarin and synthesized analogues

Compounds	IR (%) [a]		IC_{50} (nM) [b]
	50µM	10µM	
SWL-1	101.35	82.46	17.28
SWL-2	100.46	87.26	9.40
SWL-9	100.31	86.25	11.31
CP-640186	102.23	93.25	5.67
Metformin	103.89	93.22	6.09

[a]The data represent the mean values of independent experiments.
[b]IC_{50} values for ACC-2 Inhibition

3.3.2 Effect of synthesized analogues on the viability of 3T3-L1 cells

The viability assay was used to determine suitable dose and possible cytotoxic effect of synthesized analogues on adipocytes. 3T3-L1 preadipocytes were incubated in the presence of different doses of synthesized analogues SWL-1, SWL-2 and SWL-9 (10, 50, 100, 250 and 500 µg/ml) for 48 h. As shown in **Figure 4**, treatment with SWL-1, SWL-2 and SWL-9 at all tested concentrations did not cause any major toxicity.

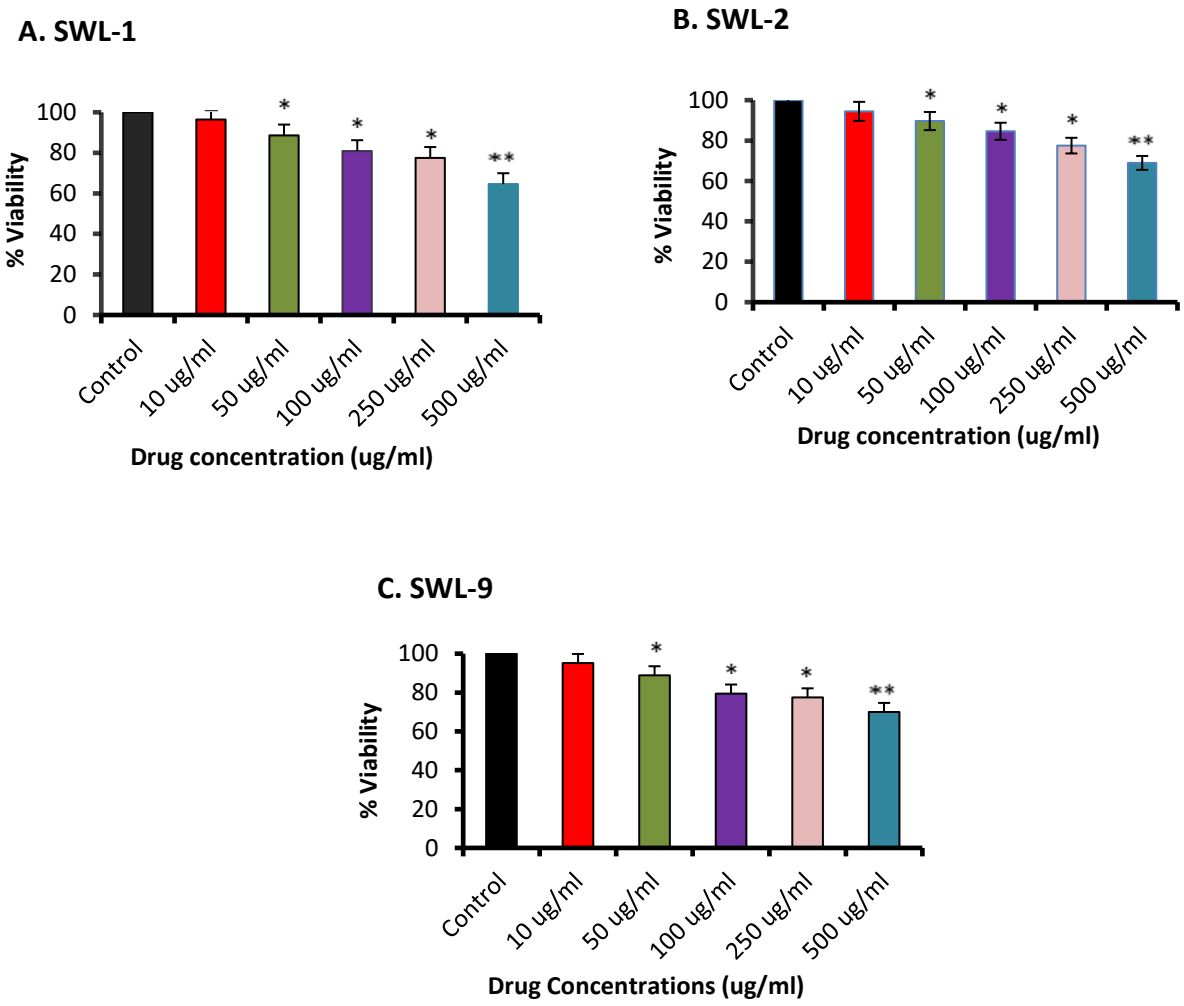

Figure 4: Effects of Swertiamarin (SWL-1) and synthesized analogues SWL-2 and SWL-9 on cell viability of 3T3- L1 cells. Data were expressed as mean ± SEM (n= 3). *P < 0.05 and **P < 0.01 vs. control group.

3.3.3 Oleic acid induced 3T3-L1 cells differentiation

In our current research, we investigated the impact of Swertiamarin and its synthetic analogues on adipogenesis using the 3T3-L1 cell model under conditions of excess fatty acid (Oleic acid). The 3T3-L1 cells are widely recognized and extensively used as a cell model for studying adipogenesis and metabolic disorders. Adipose tissue plays a vital role in maintaining fatty acid homeostasis, which is crucial for regulating energy balance. During times of caloric surplus, adipocytes store extra free fatty acids as triglycerides, and when the body experiences an energy deficit, they release stored fat. Throughout the 10-day differentiation process of adipogenesis, we closely monitored and evaluated the following parameters to assess their impact on adipogenesis at specific time points:

1. Morphological changes
2. Accumulation of lipids at the end of differentiation comparing to control cells

On the 10th day of the differentiation process, both the control cells and the cell cultures treated with oleic acid (0.5 mM) exhibited the complete adipocyte phenotype, wherein the cells contained lipid droplets distributed throughout the cytoplasm **(Figure 5)**.

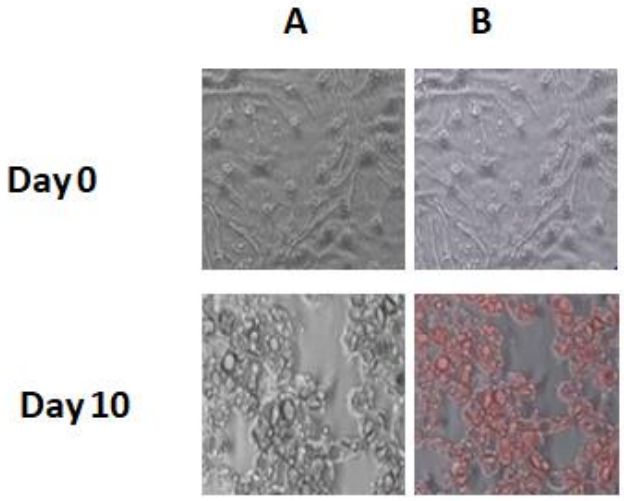

Figure 5: 3T3-L1 adipocyte differentiation. (A) Phase contrast images of 3T3-L1 cells from the start of the experiment (day 0) to ten days after the experiment. At first, the cells look like fibroblasts. During differentiation, the shape of the cell changes and lipid droplets build up inside the cell. (B) Triglyceride stained with Oil Red O on 3T3-L1 cells. At first, there isn't much staining on the fibroblast phenotype. As the adipocytes get older, they get more stained.

3.3.4 Effect of synthesized analogues on intracellular triglycerides accumulation

The fat accumulation in 3T3-L1 cells was significantly reduced when treated with SWL-1, SWL-2 and SWL-9 at a concentration of 100 μg/ml. This was observed through a noticeable decrease in the formation of lipid droplets. Additionally, the treatment with SWL-1, SWL-2 and SWL-9 resulted in a significant decrease in intracellular triglyceride accumulation when compared to the control cells treated with excess of Oleic acid and Dexamethasone **(Figure 6)**. It was essential to investigate whether the decrease in triglyceride accumulation was attributed to the inhibition of de novo lipid synthesis or an enhancement in lipolysis.

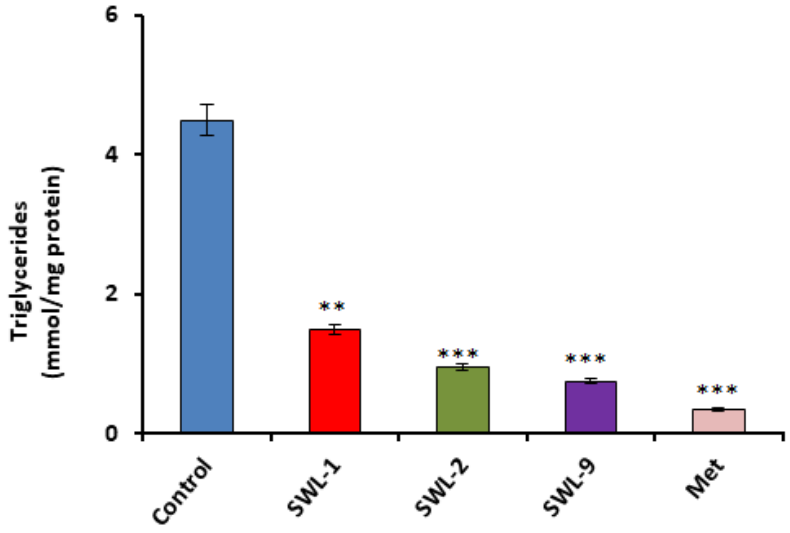

Figure 6: We quantified the build-up of triglycerides within the cell using a specialized assay kit after extracting lipids from fully differentiated 3T3-L1 cells that were cultured for a period of 10 days, as outlined in the methodology section. The data is presented as the mean ± SEM, *P < 0.05, **P < 0.01, and ***P < 0.001 vs. control group.

3.3.5 ELISA based assay estimation for ACC-2 and CPT-1

ACC-2 and CPT-1 are the potential markers associated with metabolic abnormalities such as diabetes-induced dyslipidemia and insulin resistance. We conducted a study to assess the impact of SWL-1, SWL-2 and SWL-9 on the protein expression of ACC-2 and CPT-1 on differentiated 3T3-L1 cells. Increased expression of ACC-2 has been identified as a contributor to the stimulation of lipogenesis, resulting in higher incidences of obesity and insulin resistance. Treatment with SWL-1, SWL-2 and SWL-9 (100 µg/ml) significantly decreased ACC-2 protein expression, however the extent of decrease for synthesized analogues; SWL-2 and SWL-9 was greater than SWL-1 concerning to Metformin and was shown in **Figure 7A**. All analogues; SWL-1 SWL-2 and SWL-9 significantly reduced the expression of ACC-2 compared to the control cells.

A decrease in fat accumulation can be attributed to an increase in fat breakdown and release. The expression of CPT-1, which plays a key role in fat oxidation, was measured to investigate the effect of synthesized analogues by promoting fat oxidation. Swertiamarin (SWL-1) and its synthesized analogues (SWL-2 and SWL-9) demonstrated a significant increase in CPT-1 expression **(Figure 7B).**

Furthermore, our findings revealed that all treatments significantly reduced the protein expression of ACC-2 in differentiated 3T3-L1 adipocytes compared to the control cells treated with excess of oleic acid and Dexamethasone. Consequently, inhibiting ACC-2 could serve as an effective approach in treating lipid disorders, obesity-associated dyslipidemia, and insulin

resistance. Additionally, ACC-2 negatively regulates CPT-1 activity, leading to a subsequent enhancement in the process of fatty acid oxidation.

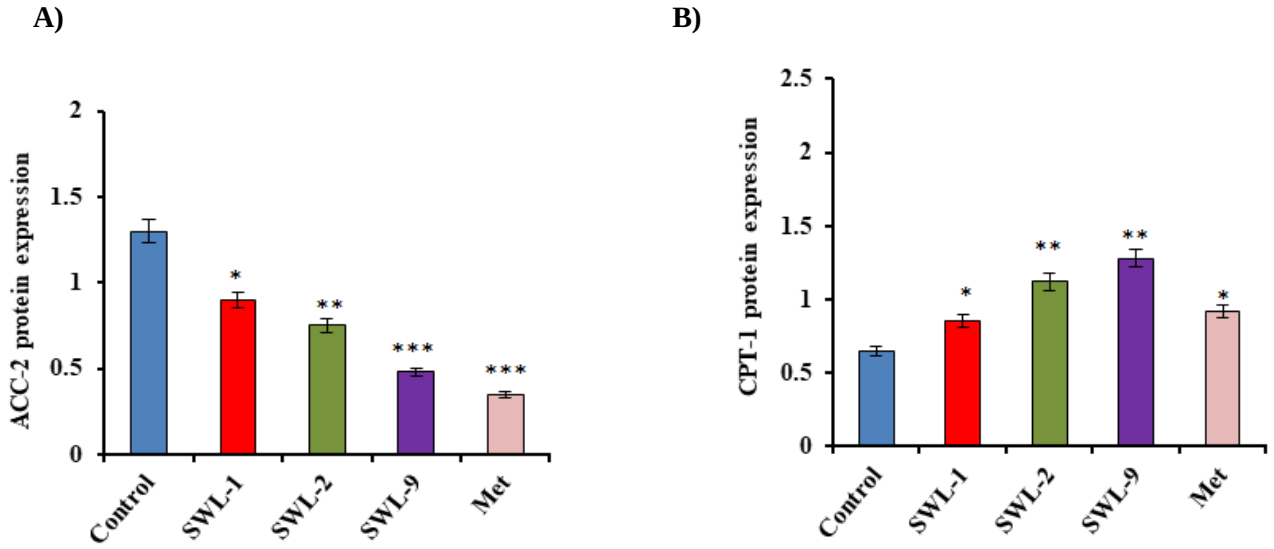

Figure 7: Evaluation of ACC-2 and CPT-1 expression in 3T3-L1 differentiated cells with the excess depletion of triglycerides. The impact of swertiamarin (SWL-1) and its synthesized derivatives (SWL-2 and SWL-9) on the protein expression related to significant metabolic conditions like diabetes and insulin resistance was investigated **A)** ACC-2 and **B)** CPT-1 in 10 day fully differentiated 3T3-L1 cells. Protein extraction done from 10 day fully differentiated 3T3-L1 cells as described in method. The results are expressed as the mean ± SEM, with statistical significance indicated by *P < 0.05, **P < 0.01, and ***P < 0.001 vs. control group.

3.4 ADMET Studies

The ADME properties of synthesized compounds were analyzed using Qikprop. The result of Qikprop analysis of synthesized compounds SWL-2 and SWL-9 are presented in **Table 4**. MM/GBSA studies of synthesized analogues against the catalytic binding pocket of Human Acetyl-CoA carboxylase 2 receptor (PDB ID: 3TDC) and Carnitine palmitoyl transferase 1 (PDB ID: 1NM8) revealed that its binding free energy is less than that of standard (Metformin), indicating that the newly synthesized analogues SWL-2 and SWL-9 may be stable in the receptor pocket **(Table 5).**

Table 4: ADMET analysis of swertiamarin analogues

S.N.	Compound Code	QP log P o/w	% HOA	Rule of Five	QP log HERG	QP P Caco	QP log BB
1.	SWL-2	0.374	40.38	2	-4.911	119.192	-2.046

2.	SWL-9	-0.545	27.06	2	-4.644	42.96	-2.61
3.	Metformin	-0.712	65.467	0	-2.983	242.686	-1.034

Table 5: MM/GBSA binding score against catalytic binding pocket of ACC-2 and CPT- 1

S.N.	**Compound Code**	**Acetyl-CoA carboxylase 2**			**Carnitine palmitoyltransferase 1**		
		Evdw[d]	**Ecoul[e]**	**ΔGbind**	**Evdw[d]**	**Ecoul[e]**	**ΔGbind**
1.	SWL-2	-37.3098	-20.1685	-39.0056	-49.521	-11.9493	-40.1614
2.	SWL-9	-39.8597	-25.6131	-51.6133	-54.3728	-12.8	-36.7562
3.	Metformin	-7.12323	-56.5311	-8.73242	-15.4806	-78.9877	-14.9602

4. Discussion

In our present work, we examined the effects of Swertiamarin and its synthetic analogues to manage diabetes-induced dyslipidemia using 3T3-L1 cell model in excess of fatty acid (Oleic acid). The 3T3-L1 cell line is widely recognized and extensively employed for studying metabolic disorders. Adipose tissue plays a crucial role in maintaining fatty acid homeostasis throughout the body, thereby controlling energy balance. During periods of calorie surplus, adipocytes store free fatty acids as triglycerides, while in times of energy deficiency, they release stored fat. Our study reveals that swertiamarin and its synthetic analogues exhibit robust anti-adipogenic effects. These compounds promote the release of stored fat and its subsequent oxidation, while simultaneously reducing fatty acid synthesis. This regulation is achieved through the modulation of CPT-1 and ACC-2 targets.

In previous studies, the anti-diabetic and anti-hyperlipidemic effects of swertiamarin in animal models were reported [13, 28]. However, it has been noted in previous reports that swertiamarin has a short plasma half-life [16]. To enhance the potency of swertiamarin, we designed and synthesized derivatives of swertiamarin such as; SWL-2 and SWL-9 to improve bioavailability and their anti-adipogenic properties using 3T3-L1 cells. Treatment with SWL-1, SWL-2 and SWL-9 resulted in a significant inhibition of adipocyte differentiation and intracellular triglyceride accumulation in 3T3-L1 cells compared to the control cells. During the process of adipogenesis, pre-adipocytes undergo morphological changes and transform into mature adipocytes through growth arrest and differentiation stimulation using a specific cocktail. By day 8-10, the cells start accumulating triglycerides and reach a terminally differentiated adipocyte state [18]. Adipocyte differentiation is a complex process regulated by various mechanisms, including transcriptional regulation through changes in the expression of adipocyte-specific

genes, such as ACC-2 and CPT-1 [16]. The protein expression of ACC-2 was significantly decreased by all treatments with SWL-1, SWL-2 and SWL-9. This decrease, along with reduced fat synthesis and accumulation, indicates that SWL-1, SWL-2 and SWL-9 possess anti-adipogenic properties. Previous reports have demonstrated that inhibiting ACC-2 in adipose tissue can protect against high-fat diet-induced obesity and insulin resistance [23]. Others have also reported inhibition of ACC-2 has been suggested as a potential target for type-2 diabetes [25].

All treatments with Swertiamarin and its synthesized analogues demonstrated inhibition of triglyceride accumulation in 3T3-L1 cells. To determine the underlying mechanism responsible for the decrease in triglyceride accumulation, we investigated whether it was attributed to the inhibition of de novo lipid synthesis or an increase in lipolysis. Our findings revealed that all treatments with SWL-1, SWL-2 and SWL-9 significantly reduced the protein expression of ACC-2 in differentiated 3T3-L1 adipocytes when compared to the control cells **[Figure 7 A &B]**. This suggests that inhibiting ACC-2 could be an effective approach for treating lipid disorders, diabetes-induced dyslipidemia, and insulin resistance. Additionally, ACC-2 negatively regulates CPT-1 activity, which subsequently enhances fatty acid oxidation [26]. CPT-1, a rate-limiting enzyme involved in fatty acid oxidation, facilitates the transport of long-chain fatty acids from the cytosol into the mitochondrial matrix [24,26]. Treatment with SWL-1, SWL-2 and SWL-9 significantly increased the protein expression of CPT-1 compared to the control cells. Notably, the increase was more pronounced for SWL-2 and SWL-9. Previous studies have also demonstrated that promoting free fatty acid transport via CPT-1 in adipose tissue and liver is beneficial for obesity management. Furthermore, research has indicated that the downregulation of ACC-2 and upregulation of CPT-1 protein expression in 3T3-L1 adipocytes contribute to the anti-adipogenic and anti-obesity effects of curcumin [27, 29]. In addition, an evaluation was conducted on the pharmacokinetic profiles of the analogues in order to ascertain their ADME characteristics. On the basis of ADME and MM/GBSA results all the synthesized analogues proved their stability as comparison to standard Metformin **[Table 4 &5]**.

Pharmacological intervention for treating lipid disorders involves two main strategies: (1) promoting the breakdown of triglycerides to reduce fat storage, and (2) enhancing the oxidation of newly released fatty acids. This approach has led to the development of beta 3-adrenergic agonists. Our research findings strongly suggest that compounds SWL-1, SWL-2 and SWL-9 exert their effects through various pathways in adipocytes. They inhibit fat uptake and synthesis while increasing fat oxidation. Therefore, these compounds, SWL-1, SWL-2 and SWL-9 have the potential to serve as anti-adipogenic agents in lipid disorders such as dyslipidemia and insulin resistance associated with diabetes.

5. Conclusions

Swertiamarin and its synthesized analogues were successfully created targeting fatty acid metabolic receptors ACC-2 and CPT-1 through molecular modelling studies. Subsequently,

ACC-2 enzymatic inhibition assay and cell-based assay were conducted on 3T3-L1 adipocytes to evaluate the efficacy of these analogues, namely SWL-1, SWL-2 and SWL-9. These analogues demonstrated significant activity against the primary targets involved in lipid metabolism, namely ACC-2 and CPT-1, when compared to the positive standards, CP-640186 and Metformin. The inhibition of ACC-2 by swertiamarin and its analogues resulted in potent anti-adipogenic effects, while simultaneously increasing fat breakdown and promoting fatty acid oxidation by upregulating the expression of CPT-1 in 3T3-L1 adipocytes. In addition, an evaluation was conducted on the pharmacokinetic profiles of the analogues in order to ascertain their ADME characteristics.

Funding: Not applicable.

Ethical approval: Not applicable.

Data Availability Statement: Not applicable.

Conflicts of Interest: The author declares no conflict of interest.

Abbreviations

ACC: acetyl-CoA carboxylase; CACT: carnitine/acylcarnitine translocase; CPT-1: carnitine palmitoyltransferase 1; CPT-2: carnitine palmitoyltransferase 2; CrAT: carnitine acetyltransferase; FAOD, fatty acid oxidation disorder; DMEM: Dulbecco's Modified Eagle's Medium; DMSO: Dimethylsulphoxide; FBS: Fetal Bovine Serum; MTT: 3-(4 5-Dimethylthiazol-2-yl)-2, 5-Diphenyltetrazolium Bromide; HRP: Horseradish peroxidase.

Acknowledgements

We express our gratitude to the Indian Council of Medical Research (ICMR), New Delhi, for their generous funding that supported the research conducted in this study. We thank to Vice Chancellor DPSRU for providing excellent infrastructure for this work.

† **Supplementary data:** The supporting information includes spectral data details (NMR and Mass) of swertiamarine and synthesized compounds.

References:

1. Morino K, Petersen KF, Shulman GI (2016) Molecular Mechanisms of Insulin Resistance in Humans and Their Potential Links with Mitochondrial Dysfunction. Diabet 55(2): 9–15. https://doi.org/10.2337/db06-s002.
2. Rotella CM, Pala L (2008) Time to insulin in type-2 diabetes: high hurdles or Santiago way?. Acta Diabetol. 45(2): 67–74. https://doi.org/10.1007/s00592-008-0027-x.

3. Zhang L, Liu Y, Wang X, Zhang X (2023) Physical Exercise and Diet: Regulation of Gut Microbiota to Prevent and Treat Metabolic Disorders to Maintain Health. Nutrient 15(6): 1539. https://doi.org/10.3390/nu15061539.
4. Koves TR, Ussher JR, Noland RC, Slentz D, Mosedale M, Ilkayeva O, Bain J, Stevens R, Dyck JR, Newgard CB, Lopaschuk GD, Muoio DM (2008) Mitochondrial overload and incomplete fatty acid oxidation contribute to skeletal muscle insulin resistance. Cell metabol 7(1): 45–56. https://doi.org/10.1016/j.cmet.2007.10.013.
5. Dambrova M, Makrecka-Kuka M, Kuka J, Vilskersts R, Nordberg D, Attwood MM, Smesny S, Sen ZD, Guo AC, Oler E, Tian S, Zheng J, Wishart DS, Liepinsh E, Schiöth HB (2022) Acylcarnitines: Nomenclature, Biomarkers, Therapeutic Potential, Drug Targets, and Clinical Trials. Pharmacological rev 74(3):506–551. https://doi.org/10.1124/pharmrev.121.000408.
6. Harwood HJ Jr. (2005) Treating the metabolic syndrome: acetyl-CoA carboxylase inhibition. Expert opi. on thera Target 9(2):267–281. https://doi.org/10.1517/14728222.9.2.267.
7. Levert KL, Waldrop GL, Stephens JM (2002) A biotin analog inhibits acetyl-CoA carboxylase activity and adipogenesis. The J. of biological chem 277(19): 16347–16350. https://doi.org/10.1074/jbc.C200113200.
8. Bruce CR, Hoy AJ, Turner N, Watt MJ, Allen TL, Carpenter K, Cooney GJ, Febbraio MA, Kraegen EW (2009) Overexpression of carnitine palmitoyltransferase-1 in skeletal muscle is sufficient to enhance fatty acid oxidation and improve high-fat diet-induced insulin resistance. Diabet 58(3): 550–558. https://doi.org/10.2337/db08-1078.
9. McGarry JD, Brown NF (1997) The mitochondrial carnitine palmitoyltransferase system from concept to molecular analysis. European j of biochem 244(1):1–14. https://doi.org/10.1111/j.1432-1033.1997.00001.x.
10. Yonezawa T, Yonekura S, Kobayashi Y, Hagino A, Katoh K, Obara Y (2004) Effects of long-chain fatty acids on cytosolic triacylglycerol accumulation and lipid droplet formation in primary cultured bovine mammary epithelial cells. J of dairy sci 87(8):2527–2534. https://doi.org/10.3168/jds.S0022-0302(04)73377-9.
11. Ma Q, Zhou X, Hu L, Chen J, Zhu J, Shan A (2020) Leucine and isoleucine have similar effects on reducing lipid accumulation, improving insulin sensitivity and increasing the browning of WAT in high-fat diet-induced obese mice. Food & func 11(3): 2279–2290. https://doi.org/10.1039/c9fo03084k.
12. Vaidya H, Rajani M, Sudarsanam V, Padh H, Goyal RK (2009) Swertiamarin: a lead from Enicostemma littorale Blume. for anti-hyperlipidaemic effect. European j of pharmacol 617(1-3): 108–112. https://doi.org/10.1016/j.ejphar.2009.06.053.
13. Vaidya H, Prajapati A, Rajani M, Sudarsanam V, Padh H, Goyal RK (2012) Beneficial effects of swertiamarin on dyslipidaemia in streptozotocin-induced type 2 diabetic rats. Phytotherapy res 26(8): 1259–1261. https://doi.org/10.1002/ptr.3708.
14. Sharma K, Tanwar O, Sharma S, Ali S, Alam MM, Zaman MS, Akhter M (2018) Structural comparison of Mtb-DHFR and h-DHFR for design, synthesis and evaluation of selective

non-pteridine analogues as antitubercular agents. Bioorganic chem 80: 319–333. https://doi.org/10.1016/j.bioorg.2018.04.022.

15. Vishwakarma S, Rajani M, Bagul M, Goyal RK (2008) A Rapid Method for the Isolation of Swertiamarin from *Enicostemma littorale*. Pharm Biol 42(6): 400-403, https://doi.org/10.1080/13880200490885095.
16. Vaidya HB, Goyal RK, Cheema SK (2014) Acetylated and propionated derivatives of swertiamarin have anti-adipogenic effects. J of pharmacol & pharmacothera 5(4): 232–238. https://doi.org/10.4103/0976-500X.142429.
17. Srivastava P, Barman J, Pathmasiri W, Plashkevych O, Wenska M, Chattopadhyaya J (2007) Five- and six-membered conformationally locked 2',4'-carbocyclic ribo-thymidines: synthesis, structure, and biochemical studies. J of the American Chem Soc 129(26): 8362–8379. https://doi.org/10.1021/ja071106y.
18. Svensson RU, Parker SJ, Eichner LJ, Kolar MJ, Wallace M, Brun SN, Lombardo PS, Van Nostrand JL, Hutchins A, Vera L, Gerken L, Greenwood J, Bhat S, Harriman G, Westlin WF, Harwood HJ Jr., Saghatelian A, Kapeller R, Metallo CM, Shaw RJ (2016) Inhibition of acetyl-coa carboxylase suppresses fatty acid synthesis and tumor growth of non-small-cell lung cancer in preclinical models. Nat Med 22:1108-1119. https://doi.org/10.1038/nm.4181.
19. Malodobra-Mazur M, Cierzniak A, Dobosz T (2019) Oleic acid influences the adipogenesis of 3T3-L1 cells via DNA Methylation and may predispose to obesity and obesity-related disorders. Lipids in health and dis 18(1): 230. https://doi.org/10.1186/s12944-019-1173-6.
20. Vaidya H, Goyal RK, Cheema SK (2013) Anti-diabetic activity of swertiamarin is due to an active metabolite, gentianine, that upregulates PPAR-γ gene expression in 3T3-L1 cells. Phytotherapy res 27(4): 624–627. https://doi.org/10.1002/ptr.4763.
21. Marks DC, Belov L, Davey MW, Davey RA, Kidman AD (1992) The MTT cell viability assay for cytotoxicity testing in multidrug-resistant human leukemic cells. Leukemia res 16(12):1165–1173. https://doi.org/10.1016/0145-2126(92)90114-m.
22. Lowry OH, Rosebrough NJ, Farr AL, Randall RJ (1951) Protein measurement with the Folin phenol reagent. The J of biological chem 193(1):265–275. https://doi.org/10.1016/s0021-9258(19)52451-6.
23. Langin D (2006) Adipose tissue lipolysis as a metabolic pathway to define pharmacological strategies against obesity and the metabolic syndrome. Pharmacol Res 53(6): 482–491. https://doi.org/10.1016/j.phrs.2006.03.009.
24. Schreurs M, Kuipers F, Van der Leij FR (2010) Regulatory enzymes of mitochondrial beta-oxidation as targets for treatment of the metabolic syndrome. Obesity rev 11(5): 380–388. https://doi.org/10.1111/j.1467-789X.2009.00642.x.
25. Tong L, Harwood HJ (2006) Acetyl-coenzyme A carboxylases: versatile targets for drug discovery. J of cellular biochem 99(6):1476–1488. https://doi.org/10.1002/jcb.21077.
26. Zang Y, Wang T, Xie W, Wang-Fischer YL, Getty L, Han J, Corkey BE, Guo W (2005) Regulation of acetyl CoA carboxylase and carnitine palmitoyl transferase-1 in rat adipocytes. Obesity res 3(9):1530–1539. https://doi.org/10.1038/oby.2005.188.

27. Peyron-Caso E, Quignard-Boulangé A, Laromiguière M, Feing-Kwong-Chan S, Véronèse A, Ardouin B, Slama G, Rizkalla SW (2003) Dietary fish oil increases lipid mobilization but does not decrease lipid storage-related enzyme activities in adipose tissue of insulin-resistant, sucrose-fed rats. The J of nutri 133(7): 2239–2243. https://doi.org/10.1093/jn/133.7.2239.
28. Dhanavathy G (2015) Immunohistochemistry, histopathology, and biomarker studies of swertiamarin, a secoiridoid glycoside, prevents and protects streptozotocin-induced β-cell damage in Wistar rat pancreas. J of endocrin Investing 38(6): 669–684. https://doi.org/10.1007/s40618-015-0243-5.
29. Ejaz A, Wu D, Kwan P, Meydani M (2009) Curcumin inhibits adipogenesis in 3T3-L1 adipocytes and angiogenesis and obesity in C57/BL mice. The J of nutri 139(5): 919–925, https://doi.org/10.3945/jn.108.100966.